Z. Physik B 24, 53–63 (1976)

Zeitschrift
für Physik B
© by Springer-Verlag 1976

Electron Spin Resonance in Superconducting Materials

K. Baberschke
Institut für Atom- und Festkörperphysik, Freie Universität Berlin

Received November 17, 1975

The ESR of Gd in the superconducting phase of the type II superconductors $CeRu_2$ and $LaOs_2$ shows a shift for the field for resonance and inhomogeneous broadening of the lineshape. Both effects strongly depend on the three different microwave frequencies (resp. magnetic fields). The broadening of max. 800 G is attributed to a non resolved fine-structure splitting. The local field distribution in vortex state of these type II superconductors is less than 100 G and is the main contribution for shift of the field for resonance. In addition ESR results of Gd and Eu doped into La are discussed for $T > T_c$. The comparison of depression of the superconducting transition temperature and exchange spin-flip scattering rate determined from ESR shows a perfect agreement.

1. Introduction

The effect of paramagnetic impurities on superconductivity has been investigated by many experimental techniques over many years. 25 years ago Buckel and Hilsch discovered the depression of the superconducting transition temperature in the presence of a magnetic impurity [1]. There are many bulk measurements of superconductors doped with many impurities [2]; there are only few direct spectroscopic measurements of the impurity states. One of the techniques which can be used to that purpose is Electron Spin Resonance (ESR). In 1973 two experiments were reported which show the linewidth and the field for resonance as a function of temperature for Gd impurities in the superconducting phase of the intermetallic compounds $LaRu_2$ [3] and $CeRu_2$ [4] (type II superconductors).

Electron paramagnetic resonance of a localized moment in a metal measures the static and dynamic transverse susceptibility. The shift of the field for resonance in a metallic environment as compared to that in a nonmetallic host matrix (e.g. CaF_2, CaO) is usually expressed as a shift of the g-factor $\Delta g = g_{\text{metal}} - g_{\text{ion}}$. This shift is caused by the polarization of the conduction electrons at the site of the paramagnetic impurity ion (local static susceptibility). The relaxation of the impurity spin between the different Zeeman levels produces a spin flip for the conduction electrons. Only those conduction electrons at the Fermi surface which can scatter into an empty state ($\alpha\, k_B T$) can contribute to the linewidth. Therefore the linewidth yields information on the dynamic susceptibility averaged over the Fermi surface. Both quantities, the g-shift and the impurity spin conduction electron relaxation rate, measured in superconducting materials, can be compared with superconducting properties. The relaxation rate is related to the initial depression of the superconducting transition temperature (T_c) produced by the impurity magnetic moment $\Delta T_c/\Delta c$ for $T_c \to T_{c0}$. (T_{c0} = transition temperature of the pure host matrix, c = impurity concentration) [5, 6]. For a long-lived local moment this depression was calculated in 1960 by Abrikosov and Gorkov [7]. In contrast to other methods (NMR, ME ...) from which the relaxation rate also can be extracted, the ESR measures (in case of a bottleneck system) the spin flip scattering rate directly. The bare experimental results can then be compared directly with the experimental depression of the transition temperature – even without using the density of states for the conduction electrons from other experiments.

For the determination of the relaxation rate ($T > T_c$), in principle all superconducting materials can be investigated, but as most of the experiments are per-

formed in polycrystalline samples, the cubic metals and intermetallic compounds are favoured. Here we focus on La metal (fcc phase) and $LaAl_2$. The resonance of Eu and Gd doped into La (fcc) has most recently been detected [8]. This and the $LaAl_2$ [5, 9] are bottlenecked, which makes a correlation to superconductivity especially interesting.

To detect the ESR signal *in* the superconducting phase ($T<T_c$), type II superconductors with an upper critical field $H_{c2}>H_0=3$ to 12 kG are needed. These are the A 15 (V_3X) and the C 15 ($CeRu_2$, $LaRu_2$, $LaOs_2$) compounds. Most of the other high field superconductors have a more complicated lattice structure and many of them are nonstoichiometric compounds. The A 15 are metallurgically much more difficult to prepare. Therefore all of the published ESR experiments – for $T<T_c$ – reported up to now use the C 15 compounds as a host metal.

2. ESR in Metals

The theory of ESR in metals has been reviewed thoroughly [10]. Here only the most important results will be repeated to facilitate the reading of the experimental section. The Hamiltonian of very dilute localized moments in a metallic host (e.g. 100 ppm Gd in La) in an applied field can be written

$$\mathcal{H}=\mathcal{H}_{\text{ion}}+\mathcal{H}_e+\mathcal{H}_{\text{int}}.$$

$\mathcal{H}_{\text{ion}}$, the Hamiltonian of the ion in an ionic host matrix, is given by

$$\mathcal{H}_{\text{ion}}=-g_{\text{ion}}\,\mu_B\,H_0\,S_z+\mathcal{H}_{\text{C.E.F.}}+\mathcal{H}_{il}.$$

Here we use **S** instead of **J** because most of the experiments are performed with S-state ions (Gd^{3+}, Eu^{2+}). The g-factor in ionic hosts like in CaF_2 equals for Gd $g_i=1.992(1)$. For $S>1/2$ the paramagnetic impurity interacts also with the crystalline electric field (C.E.F.). The experiments discussed in the present paper ($S=7/2$, 7 lines) show mostly a single line spectrum because all the fine structure lines are collapsed. Therefore we neglect for a moment $\mathcal{H}_{\text{C.E.F.}}$.

The third term is the interaction between the ion and the lattice (phonons). This leads to a relaxation rate $\delta_{il}\approx 10^5\,\text{s}^{-1}$, which is small compared to all other rates we shall discuss.

For the Hamiltonian of the conduction electrons (C.E.) we get

$$\mathcal{H}_e=\mathcal{H}_{\text{kin}}-g_e\,\mu_B\,H_0\,\sigma_Z+\mathcal{H}_{\text{el}}.$$

$\mathcal{H}_{\text{el}}$ is the Hamiltonian describing the conduction electron phonon interaction; the relaxation rate for transitions between the spin levels $\langle\sigma_Z\rangle=\pm\frac{1}{2}$ is δ_{eL} and generally of the order of 10^{11}–$10^{13}\,\text{s}^{-1}$. The only interaction in an undoped metal (e.g. pure Au) which makes those processes possible is the spin orbit interaction of the conduction electrons: The spin flip scattering rate δ_{eL} causes the linewidth at low temperature in a conduction electron spin resonance experiment CESR. For $g_e\approx 2$ a linewidth of $H=300$ G corresponds to $\delta_{eL}=20^9\,\text{s}^{-1}$; therefore if δ_{eL} is some orders of magnitude larger, the CESR cannot be detected. Furthermore in doped metals the static susceptibility of the impurities χ_i is large compared to the spin susceptibility χ_e of the conduction electrons. Then in solving the two coupled resonance systems the resonance for the conduction electrons can safely be neglected.

The interaction Hamiltonian $\mathcal{H}_{\text{int}}$ between the impurity spin system and the conduction electron system is written in the form

$$\mathcal{H}_{\text{int}}=-J\,\mathbf{S}\,\boldsymbol{\sigma}.$$

This is an oversimplification assuming that the exchange interaction is isotropic, δ-function like, containing only one contribution, etc. To explain experiments like specific heat data, resistivity results in Kondo systems, or depression of superconducting transition temperature, this very simple form of the exchange interaction is used. Also in this paper we will simplify the exchange coupling between the conduction electrons and the localized moment, but in contrast to other experimental techniques the ESR on a localized spin in a metallic matrix independently measures in two ways the exchange interaction:

1) to determine the *field for resonance* or the corresponding *g-factor* we use the Hamiltonian

$$\mathcal{H}_{\text{eff}}=-(g_i\,\mu_B\,H_0\,S_z+J\,\mathbf{S}\,\boldsymbol{\sigma})$$

H_0, the applied field, determines the z-axis. The resonance frequency is then given by

$$|\hbar\,\omega|=g_i\,\mu_B\,H_0\,S_z+JS_z\langle\sigma_Z\rangle.$$

The exchange interaction J times the magnetization of the conduction electron $\langle\sigma_Z\rangle$ produces an internal field at the impurity site. This is expressed in terms of a g-shift

$$\Delta g=J\cdot N(E_F),\qquad J\gtrless 0;\ \Delta g\gtrless 0. \tag{1}$$

Here a free electron gas was assumed yielding $g_e\,\mu_B\langle\sigma_Z\rangle/H_0=N(E_F)\,\mu_B^2$. This g-shift is temperature and concentration independent. At higher concentrations ($\approx 1\,\%$) and low temperature, internal field contribution by a RKKY interaction between magnetic impurities may occur. This can be avoided by diluting the system.

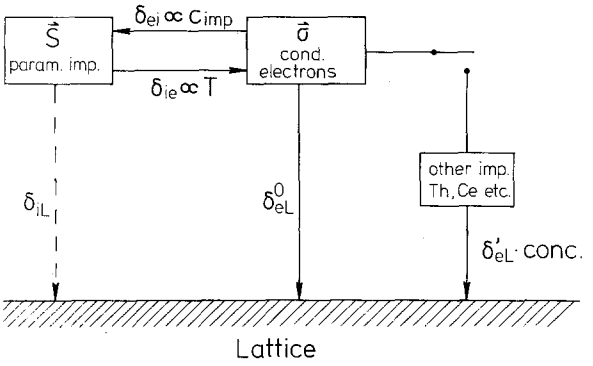

Fig. 1. Different relaxation paths between the coupled resonance system (paramagnetic impurity and conduction electron) and to the thermal bath. $\delta'_{el} = \partial_{el}/\partial c_{imp}$

2) *The relaxation rate* (spin-flip) from the localized moment to the conduction electron δ_{ie} and vice versa δ_{ei} are in a first Born approximation proportional to the exchange interaction squared. Only the conduction electrons at the Fermi surface can participate in those spin flip processes. Therefore the relaxation in an ESR experiment determines $\langle J^2(\mathbf{k}, \mathbf{k}')\rangle_{\text{F.S.}}$. $\mathbf{k}/\mathbf{k}'$ are the in/out wave vectors of the conduction electrons. $|k| = |k'| = k_F$.

$$\hbar\delta_{ie} = \begin{cases} \pi N^2(E_F)\langle J^2(k,k')\rangle\, kT & \omega_0 < kT \text{ (Korringa)} \\ \pi N^2(E_F)\langle J^2(k,k')\rangle \dfrac{S}{2}\omega_0 & \omega_0 > kT. \end{cases} \quad (2)$$

In the low temperature limit the rate is temperature independent but proportional to the microwave frequency ω_0 (10 GHz $\hat{=}$ 0.5 K).
The scattering in the reversed direction is given by

$$\hbar\,\delta_{ei} = \pi N(E_F)\langle J^2(k,k')\rangle\, 2S(S+1)\cdot c_{imp}. \quad (3)$$

Both quantities are well known from NMR. δ_{ie} corresponds to the "Korringa-rate" and δ_{ei} to the "Overhauser-rate". They are related in the "detailed balance" condition to the susceptibility of the two subsystems [11, 12].

$$\chi_i/\chi_e = \delta_{ei}/\delta_{ie}. \quad (4)$$

Figure 1 shows schematicly the different relaxation rates. Assuming (RE impurities) $J \approx 0.1$ eV and $N(E_F) \approx$ 1/eV spin, we get at $T = 1$ K $\delta_{ie} = 10^9\ \text{s}^{-1}$ and for a concentration of the localized moments of $c_{imp} \approx$ 10 ppm: $\delta_{ei} = 10^9\ \text{s}^{-1}$. This rate is approximately two orders of magnitude smaller than δ_{eL} ($= 10^{11}$ to $10^{13}\ \text{s}^{-1}$). Under those conditions the subsystem of the conduction electrons is in thermal equilibrium with the lattice (Fig. 1).

Case 1. Isothermal ($\delta_{ei} \ll \delta_{eL}$)

The thermal broadening of the linewidth DH yields

$$g\,\mu_B DH_{\text{therm}} = \hbar\,\delta_{ie}; \quad \Delta g_{\text{exp}} = \Delta g_{\text{max}} = JN(E_F). \quad (5)$$

Experimentally one observes in addition a residual linewidth characterized by a constant "a".

$$DH_{\text{exp}} = a + bT; \quad b = \frac{d(DH)}{dT} = \frac{\hbar\,\delta_{ie}}{g\,\mu_B T}. \quad (6)$$

Case 2. Bottleneck ($\delta_{ei} \gtrsim \delta_{eL}$)

For higher impurity concentration (e.g. $c_{imp} \approx 1\,\%$) δ_{ei} may be of the same order of magnitude as δ_{eL}. Then the subsystem of the conduction electrons is no longer in thermal equilibrium with the lattice. The effective relaxation rate δ_{ie} is reduced. This was first calculated by Hasegawa and has been proven by many experiments.
Assuming $g_i \approx g_e$, the theory yields [11]

$$DH = \delta_{eL}/(\delta_{ei} + \delta_{eL})\, DH_{\text{therm}} \quad (7)$$

$$\Delta g = \left(\frac{\delta_{eL}}{\delta_{ei} + \delta_{eL}}\right)^2 \Delta g_{\text{max}}. \quad (8)$$

Here we neglect the "dynamic term". This bottleneck behaviour complicates the experiments because the dilute alloy has to be measured as a function of temperature *and* as a function of impurity concentration. Decreasing concentration of the paramagnetic impurity reduces the spin flip scattering rate of the conduction electron to the paramagnetic impurity. Therefore it breaks the bottleneck and brings the system into the isothermal case. But not only decreasing concentration of the paramagnetic spin breaks the bottleneck, also an increasing spin flip scattering rate of the conduction electrons to the lattice δ_{eL} can break the bottleneck. This can be realized by doping "dirt" into the host matrix [13]. Fitting the concentration dependence of the linewidth and the g-shift enable us to determine both relaxation rates δ_{ei}, δ_{eL}. This is a fundamental difference compared to the hyperfine coupling of a nuclear spin to the conduction electrons. Because of the weakness of the hyperfine coupling the conduction electrons are always in thermal equilibrium with the lattice.

3. Determination of the Spin Flip Scattering Rates

These rates are the controlling parameter for pair breaking or -weakening in the superconducting state. The local moments in metals can be classified [14] by their lifetime τ_{sf} compared to the thermal fluctuation lifetimes $\tau_{th} = h/k_B T$. 1. $\tau_{sf} \gg \tau_{th}(T_c)$ and $J > 0$ (e.g.

(LaGd)Al_2, LaGd); 2. $\tau_{sf} \gg \tau_{th}(T_c)$ but $J<0$ (e.g. (LaCe)Al_2, LaCe); 3. $\tau_{sf} \ll \tau_{th}(T_c)$ (e.g. ThU, ThCe).
For ThU the local moment fluctuation corresponds to a temperature of the order of 100 K ($\gg T_c \approx 1.4$ K). This is several orders of magnitude too fast to be detected by ESR. Therefore we discuss only Case 1 and Case 2. As shown in the previous chapter for the interpretation of ESR experiments one has to distinguish between the bottleneck and nonbottleneck systems.

3.1. Bottleneck System

Case 1. The admixture of the conduction electrons into the localized impurity states is small. The lifetime of an electron in the localized impurity state remains infinite. The dominating contribution to the exchange interaction between the impurity states and the conduction electrons is the Heisenberg contribution J_{atm} [2, 15], which is positive (ferromagnetic), $J_{atm}>0$. The theory by AG [7] describes very well the lowering of the superconducting transition temperature $T_c(c_{imp})$:

$$\ln(T_c/T_{c0}) = \psi(1/2) - \psi\left(1/2 + 0.14 \frac{\alpha}{\alpha_{cr}} \frac{T_{c0}}{T_c}\right).$$

The pair breaking parameter α, and its critical value α_{cr}, where superconductivity is completely destroyed, are given by the theory in the first Born approximation

$$4\hbar\,\alpha_{cr} = k_B T_{c0}/\gamma$$
$$4\hbar\,\alpha = C_{imp} N(E_F) J^2 S(S+1). \qquad (9)$$

This pair breaking parameter is within this approximation identical to δ_{ei}, the spin flip scattering rate of the conduction electron at the localized moment. This scattering destroys the superconductivity because the presence of a localized moment breaks the time reversal symmetry. As shown in the previous chapter, the rate δ_{ei} can be measured in case of a bottleneck system without any assumption of the density of states or other quantities.

$$\left|\frac{dT_c}{dc_{imp}}\right| = \frac{3\hbar\pi}{16 k_B} \frac{d\delta_{ei}}{dc_{imp}}. \qquad (10)$$

At present there are only two superconducting systems known with bottleneck behaviour: Gd or Eu doped into $LaAl_2$ [5, 9] and La [8, 16]. Figure 2 shows the experimental g-value as a function of reciprocal Gd concentration (lower scale and full dots). This and the fit of the linewidth (Equation (7)) as a function of the reciprocal Gd concentration determines the two parameters δ_{ei} and δ^0_{eL}. The best fit (b) yields $\delta_{ei} = 9 \cdot 10^{11}\ s^{-1}/1\%$ and $\delta^0_{eL} = 7 \cdot 10^{11}\ s^{-1}$. Using (10) we calculate from these data a depression of T_c: $dT_c/dc(\mathrm{ESR}) = 4.1$ K/%. The experimental value of

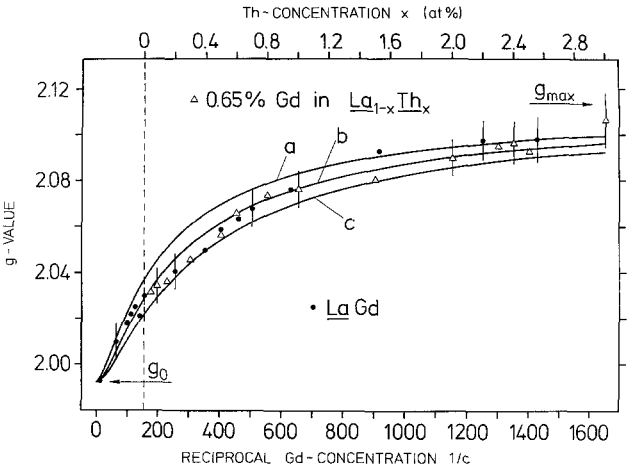

Fig. 2. The full dots show the shift of the resonance field for Gd in pure La as a function of reciprocal Gd concentration. The open triangles show the shift for a fixed Gd concentration (0.65%) as a function of the additional Th concentration. The full lines are calculated by using Equation (8), $\delta^0_{eL} = 7 \cdot 10^{11}\ s^{-1}$ (a) $\delta_{ei} = 11 \cdot 10^{13}\ s^{-1} \cdot c$ (b) $\delta_{ei} = 9 \cdot 10^{13}\ s^{-1} \cdot c$ and (c) $\delta_{ei} = 7 \cdot 10^{13}\ s^{-1} \cdot c$

our samples equals 4.0 K/% (Table 1). Adding nonmagnetic impurities like Th into the host material, one increases $\delta_{eL} = \delta^0_{eL} + \delta'_{eL} \cdot c_{dirt}$. The bottleneck can be broken by the additional s.o. scattering. Again Figure 2 shows for a fixed Gd concentration of 6,500 ppm the change of the experimental g-factor by adding Th into the host (open triangles and upper scale). The perfect agreement of both experiments with the Hasegawa equations (7) and (8) speaks for itself. The additional spin orbit scattering rate of Th was determined to be $24 \cdot 10^{11}\ s^{-1}/\%$. The measured depression of T_c caused by alloying Th into La only yields 0.2 K/%. This very nicely demonstrates that s.o. scattering does not destroy superconductivity (the corresponding number using Equation (10) and $24 \cdot 10^{11}\ s^{-1}/\%$ would be ≈ 10 K/%). This spin orbit spin flip rate is of interest; it was calculated by Yafet [17] using the nonmagnetic virtual bound state parameters.

Case 2. Here the admixture of the conduction electrons into the localized impurity states is moderately strong. Watson et al. [18, 15] showed that a second contribution to the exchange interaction a "covalent mixing" J_{cm}, becomes comparable to J_{atm}. According to Schrieffer and Wolff [19], this contribution can be calculated using the parameters of the Friedel-Anderson model [20]:

$$|J_{cm}| = \frac{\langle V_{kl} \rangle U}{E_l(E_l+U)}; \quad J_{cm}<0$$
$$J_{eff} = J_{atm} + J_{cm}. \qquad (11)$$

Table 1. Relaxation rates and depression of T_c. The numbers in parenthesis are the error bars of the last digit. dT_c/dc (ESR) is calculated from Equation (10). The numbers of LaEu are extracted only from the change of the g-shift (Eq. (8)) no good data of the thermal broadening are available

	δ^0_{eL}	δ'_{eL}	δ_{ie}/T	δ_{ei}	$\left.\frac{dT_c}{dc}\right\|_{ESR}$	$\left.\frac{dT_c}{dc}\right\|_{exp}$
	$10^{11}\,s^{-1}$	$10^{11}\,s^{-1}/\%$	$10^{9}\,s^{-1}$	$10^{11}\,s^{-1}/\%$	K/%	K/%
LaGd[a]	7(2)	(1)	1.3(2)	9(2)	4.1	4.0(2)
LaEu[b]	7(2)	–	–	(9)	(4.1)	2.1(2)
$La_{1-x}Th_xGd$[b]	7(2)	24	–	–	–	0.2(1)
$La_{1-x}Ce_xGd$[b]	7(2)	10	–	–	–	1.47(3)
$LaAl_2Gd$[c]	5(2)	–	1.1(1)	9(2)	4.1	4.0(2)
$LaAl_2Eu$[d]	5(2)	–	0.5(1)	6(2)	2.7	2.5(1)

[a] Ref. 8 [b] Ref. 16 and to be published [c] Ref. 5, 9 [d] Ref. 5, 16

E_l and V_{kl} denote the local l (d or f) state energy relative to E_F and the mixing matrix element with the itinerant states. U is the intra-atomic Coulomb repulsion of the spin-up and spin-down states. J_{cm} can be neglected for Gd because here E_f is approximately 8 eV below the Fermi level, but for $4f^1$ or $4f^{13}$ configuration (Ce or Yb) the $4f$ level is only several meV below the Fermi level. Here $|J_{cm}|$ is in the same order of magnitude or larger than J_{atm}, then J_{eff} becomes negative. This was shown for AuYb. ESR experiments show that the g-shift was negative, $\Delta g<0$ [21]. After getting this result a Kondo anomaly in the resistivity was found [22].

We focus on LaCe and (LaCe)Al_2. In both systems Ce still has a well localized moment. But the effective exchange interaction $J_{eff}=J_{atm}+J_{cm}$ is negative. In a cubic crystal field Ce splits into a Γ_7 and Γ_8. Here Γ_7 is the ground state and Γ_8 the excited one. In principle it should be possible to detect both resonances even in polycrystalline samples. As a matter of fact several groups tried to detect them without success. The reason is still unclear, especially because we show in the following that the effective relaxation rate is of the same order of magnitude as Gd.

In the absence of the expected resonance signal one can add the Ce impurities into the host and detect the change of the Gd resonance, similar to the nonmagnetic Th. This has been shown previously by D. Davidov et al. [23] for Gd(LaCe)Al_2. Here we give the corresponding data for (LaCe)Gd. The experimentally detected spin flip relaxation rate is in a first approximation the sum of (1) the *spin orbit* spin flip rate due to the admixture of the CE with nonmagnetic core states of the Ce plus (2) the *exchange* spin flip scattering of the conduction electrons with the magnetic "part" of the Ce. This latter effect also depresses T_c. However, for $J<0$ the pair breaking parameter must be calculated beyond the second order of J. According to Müller-Hartmann and Zittartz [24] this leads to a temperature dependence of α/α_{cr}. The ESR experiment measures only scattering rates for $c_{imp}\to 0$. Cornut and Coqblin [25] calculated this relaxation rate taking into account the scattering rate due to the proximity of the $4f$ level to the Fermi level and the crystalline field effect. In a low temperature limit their calculation yields

$$\hbar\delta=\frac{\pi}{2}c_{imp}N(E_F)J_{00}^2A_{00} \tag{12}$$

$$k_B\frac{dT_c}{dc}=\frac{\pi^2}{8}N(E_F)J_{00}^2\frac{\lambda_0^2-1}{(2j+1)}. \tag{13}$$

J_{00} is the exchange integral corresponding to the ground state (here Γ_7), A_{00} is the constant (tabulated in Reference 25) depending on λ_0 the degeneracy of the ground state and $j=5/2$. In Table 1 the effective relaxation rate $\delta'_{eL}=\delta_{eL}(\text{s.o.})+\delta_{eL}(\text{exchange})$ is given. Comparison with the experiment yields $\delta_{eL}(\text{s.o.})=6\cdot 10^{11}\,s^{-1}/\%$ and $\delta_{eL}(\text{exchange})=4\cdot 10^{11}\,s^{-1}/\%$. Very recently detailed measurements have been performed for the (La, Th)Ce system [26]. Ce undergoes a magnetic-nonmagnetic transition in changing the host matrix from La to Th. Approximately at $La_{0.85}Th_{0.15}$ the system shows a re-entrant behaviour in superconductivity. The scattering rates given in Table 1 (rows 3 and 4) give supplementary information only for a La host with a small concentration (1 to 2%) of Th or Ce. ESR experiments on a solid solution like $La_{0.85}Th_{0.15}$ are very sensitive to crystalline field effects, in such a solution the local symmetry of a Gd or Ce ion is no longer cubic.

In this chapter we showed how the different relaxation rates determined by ESR can be related to the depression of the superconducting transition temperature. Several effects were neglected, but all of them give minor contributions.

Table 2. Thermal broadening b and depression of T_c of Gd in the high-field superconductors. dT_c/dc (ESR) was calculated using Equation (4). For comparison the data for $LaAl_2$ and La are listed again. See also Ref. 27

Gd in		$LaOs_2$[a]	$CeRu_2$[b]	$LaRu_2$[c]	$LaAl_2$	La(fcc)
b	G/K	7.5(1.0)	10(2)	25(3)	65(5)	75(5)
$\left.\frac{dT_c}{dc}\right\|_{ESR}$	K/%	0.20	0.5	1.3	4.0	4.0
$\left.\frac{dT_c}{dc}\right\|_{exp}$	K/%	0.16(10)	+0	0.3	4.1	4.1

[a] Ref. 28 [b] Ref. 4, 29, 30 [c] Ref. 3, 29, 30

1) Depending on H_0 and DH for Ce there will be a small but finite contribution of the relaxation spectrum *at* the resonance frequency ω_{Gd}. These Ce ions are in resonance condition and modify the effective δ_{ei}.
2) On the other hand Gd not only acts as a resonance ion; there is also a dissipative contribution to the relaxation $\delta'_{eL} \cdot c_{Gd}$. Davidov et al. [23] have determined this δ'^{Gd}_{eL} for (LaGd)Al_2. Our own experiments give an upper limit of $\delta'^{(Gd)}_{eL} \leqq 1 \cdot 10^{11}\ s^{-1}/\%$ for both systems LaGd and (LaGd)Al_2. This would modify δ^0_{eL} and δ_{ei} slightly, *but only within the error bars of the given numbers.*

3.2. Nonbottlenecked Systems

In the previous chapter we described the only two superconducting host materials which show a bottleneck behaviour in our resonance experiment. Most of the other superconductors are nonbottlenecked. In some cases δ_{eL} is large compared to δ_{ei} because the host is "dirty" or non-*s*-like conduction electrons relax faster with the lattice. On the other hand δ_{ei} can be very small because of a small density of states at the Fermi energy or small exchange interaction. In all these cases δ_{ei} can be determined by using the detailed balance condition $\delta_{ei} = (\chi_e/\chi_i) \cdot \delta_{ie}$. In principle χ_e/χ_i are known and δ_{ie} can be measured. Unfortunately in practice the knowledge of both of these quantities is very poor. χ_i is only known from macroscopic measurements and χ_e is also very difficult to extract from an experiment because of spin, orbit and Van-Vleck-like contributions to the susceptibility. Using (2) only the density of states has to be known to calculate (3). In absence of better information in some publications $N(E_F)$ from specific heat experiments was used, but in the presence of electron-electron enhancement this also leads to incorrect numbers.
Nevertheless the comparison in Table 2 of the thermal broadening b (6) and the experimental dT_c/dc shows a systematic effect: the smaller the thermal broadening, the weaker the depression of the superconducting transition temperature. $LaRu_2$ shows a clear decrease of T_c, but for $LaOs_2$ and $CeRu_2$ dT_c/dc is zero within the error bars. For very small depression of the superconducting transition temperature, quantitative comparison is impossible because "nonmagnetic" effects also change T_c. In the case $CeRu_2$ the change of the valency (Gd^{3+} on a Ce^{4+} place) might increase T_c and outweigh the depression by the exchange interaction. The experimental depression of the transition temperature in Table 2 might differ slightly from numbers in the literature. Our numbers were determined from the same samples which were used for the ESR experiment. The selection between cristallographic good and bad samples was given by the sharpness of the transition width. Only those samples which showed a superconducting transition width of $\delta T_c < 0.02$–0.03 K were used for the ESR experiments. For these samples the numbers given in Table 2 are valid.
Finally the numbers given in Tables 1 and 2 can be used to determine the spin orbit mean free path $l_{s.o.}$. This is especially interesting for the high field superconductors described in the following chapter. These are nonbottlenecked systems which give a lower limit for $\delta^0_{eL} > 10^{14}\ s^{-1}$. Using $E_F \approx 7$ eV and an effective mass of $M' \approx (2 \text{ to } 4)\, M_e$ we get $l_{s.o.} < 70$ Å.

4. Gd-Resonance in the Superconducting Phase

Previous experiments show in the superconducting phase a temperature dependent shift of the field for resonance, a narrowing of the linewidth and a deviation from the Lorentzian line shape. Most of these experiments were performed only at one microwave frequency and with one host material. In this paper we present these experiments completely, showing measurements on $LaOs_2$ and $CeRu_2$ at three microwave frequencies (9 GHz (X), 24 GHz (K) and 35 GHz (Q)). This enables us to distinguish between a field dependent shift of the field for resonance and a change of the conduction electron spin susceptibility in the

Table 3. Superconducting properties of the high critical field C-15 compounds. In the dirty limit $\xi_0^2 = \phi_0/2\pi H_{c2}(0)$. For simplicity we do not distinguish between the different κ's of the GLAG theory. The upper critical field of $CeRu_2$ given in the Table is the value for our samples, it is smaller than given in literature

		$CeRu_2$	$LaOs_2$	$LaRu_2$
T_{c0}	K	6.28	9	4.5
$H_{c2}(0)$	kG	50(5)	30(3)[a]	24(3)
ξ_0	Å	70	100	110
$H_c(0)$	kG	1.2	1.6	0.8
κ_5		28	13	21
λ	A	2,200	1,300	2,300
Δg_{field} for	3.3 kG	−0.02	−0.05	
	8.5 kG	−0.006	−0.014	
	12.5 kG	−0.003	−0.008	

[a] Ref. 28

superconducting phase. Furthermore we show different behaviour in the line shape for different microwave frequencies.

In Table 3 some superconducting properties are listed. The numbers for $LaRu_2$ are given for comparison. Because this system undergoes a phase transition for $T < 30$ K into a tetragonal phase [31] the ESR is much more difficult to interpret. Furthermore the upper critical field is only 24 kG. For the same reason we omit $ThRu_2$. Here also the upper critical field is very low [33].

4.1. Shift of the Field for Resonance and Change in the Line Shape

The recorder trace in the middle of Figure 3 at $T = 7.4$ K is a signal in the normal conducting phase. The crosses show the calculated signal of a superposition of absorption and dispersion from a Lorentzian line shape (Dysonian line shape). The agreement between experiment and calculation is good. The upper and lower recorder trace are detected in the superconducting state. The resonance deviates from the normal conducting line shape (see also Figure 4). A determination of the line width and the field for resonance becomes uncertain, but the central part of the resonance signal still looks like a narrow Lorentzian line. As mentioned in Chapter 1 a $S = 7/2$ resonance contains seven lines. If we assume for the following that this narrow central line is the $1/2 \leftrightarrow -1/2$ transition, we are able to determine an effective g-value: $\hbar\omega = g\mu_B H$. This "g-value" might not be the "true" one, because the local field in the vortex state of a type II superconductor is not equal to the external [32, 35]. Figures 5 and 6 show the so-determined g-values for $LaOs_2$ and $CeRu_2$. The large error bars include all systematic errors; the smaller ones, the statistical error.

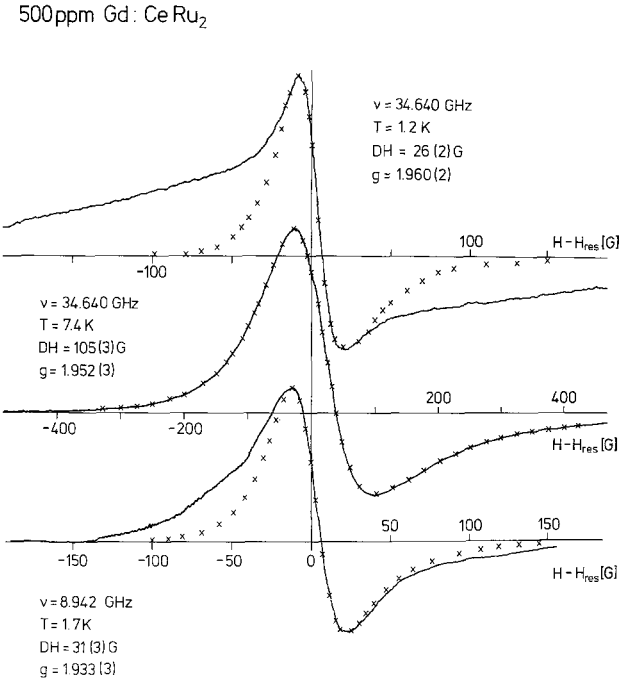

Fig. 3. The Gd resonance signal in $CeRu_2$. Experiments with different concentrations ($c_{\min} \approx 80$ ppm) show no significant difference. The broadening of the lineshape at K-band is smaller than is Q- but bigger than at X-band. The crosses are a calculated Dysonian line

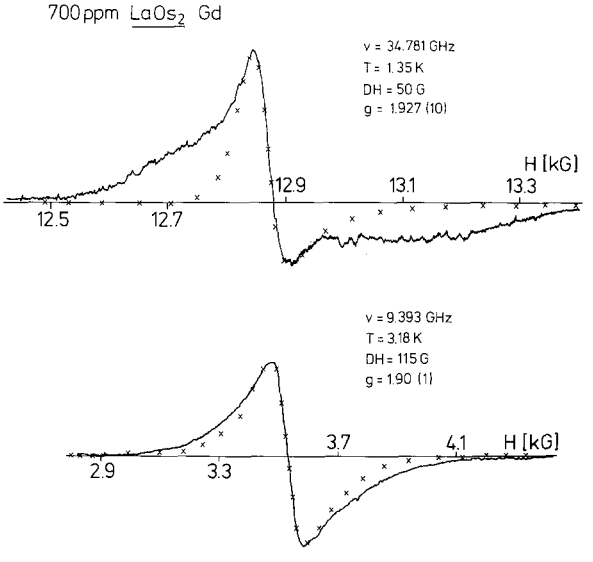

Fig. 4. The Gd resonance signal in $LaOs_2$. The lowest detected concentration was 120 ppm

NMR experiments in Vanadium and other metals [32] demonstrate very well this field distribution in a vortex state. There exist three characteristic fields, the maximum field at the vortex center H_V, the minimum field $H_{\min}$ at the center of gravity in the triangles, and

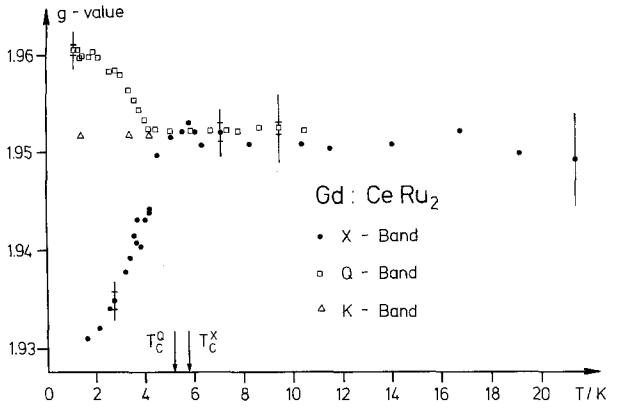

Fig. 5. Change of the field for resonance. In the normal conducting phase there is a temperature independent g-value of $g^n = 1.952(5)$. The experiments were performed on different Gd concentrations between 80 and 2,000 ppm. $T_c^{X,Q}$ denotes the appropriate transition temperature for the different applied fields

the most probable field at the saddle point H_S. Abrikosov calculated the field distribution to be

$$H_V - H_{\min} \approx \frac{H_{c2}(T) - H_0}{2\kappa^2 - 1} < H_{c1} \tag{14}$$

and

$$H_S \approx H_V - 0.9(H_V - H_{\min})$$

and Lasher the distribution function $\rho(H)$, which shows a logarythmic divergence at H_S [32]. We assume that the majority of the Gd "see" this saddle point field (statistical distribution). Using the numbers of Table 3, Equation (14) yields for $CeRu_2$ a field shift $H_{\text{normal}} - H_S$ of approximately 20 G–30 G (Q-band to X-band). The corresponding change in the g-factor is given in the last row of Table 3. The corresponding field shift for $LaOs_2$ is 50–75 G.

In these experiments mainly we were not interested in verifying this internal field distribution but in looking for the change of the spin susceptibility in the superconducting phase. Anderson [34] calculated this in the presence of strong spin orbit scattering:

$$\frac{\Delta g^n - \Delta g^s(0)}{\Delta g^n} = \frac{\chi^n - \chi^s(0)}{\chi^n} = \begin{cases} \frac{2}{\pi}\frac{l_{s.o.}}{\xi_0}; & l_{s.o.} < \xi_0 \quad (15a) \\ 1 - \frac{\pi}{6}\frac{\xi_0}{l_{s.o.}}; & l_{s.o.} > \xi_0. \quad (15b) \end{cases}$$

In the previous chapter we showed that $l_{s.o.}$ is in the same order of magnitude as the coherence length ξ_0. Under these conditions the reduction of the spin susceptibility is very small. Figure 7 shows how both effects, the reduction in spin susceptibility and the change of the local field with respect to the external one result in an effective "g-shift". The use of three different microwave frequencies shows clearly in Figures 5 and 6 that the socalled "g-shift" is strongly dependent on the applied field. Both effects work in the opposite direction and mostly the pseudoshift caused by the internal field distribution in the vortex states overcomes the reduction of the g-shift from Equation (15). On the other hand Figure 5 shows at Q-band a reduction of Δg_{exp}. This can only be caused by the change of the susceptibility. Therefore both effects are clearly present. In a quantitative analysis the uncertainties of the superconducting parameter (Table 3) and the difficulties of interpreting the central line as the $1/2 \leftrightarrow 1/2$ transition (see below) both enter. Nevertheless a rough approximation for both systems yields a spin susceptibility reduction of 13%. Using Equation (15) we get $l_{s.o.}/\xi_0 \approx 0.6$ (15a) or $\xi_0/l_{s.o.} \approx 0.3$ (15b). Both results are in reasonable agreement with other estimations of this spin orbit scattering path.

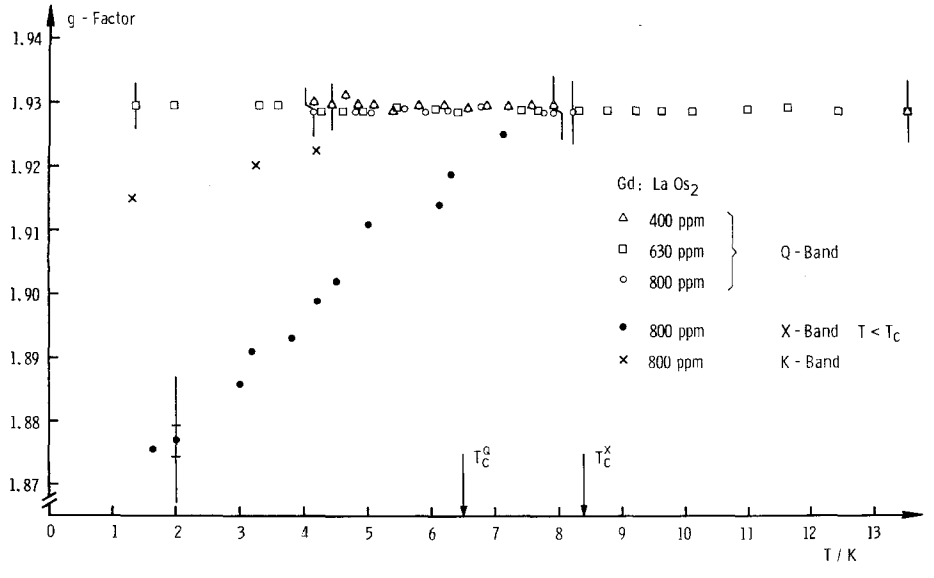

Fig. 6. Change of the field for resonance for $\underline{LaOs_2}Gd$. Because of the smaller $H_{c2}(0)$, T_c^Q and T_c^X differ more than in Fig. 5

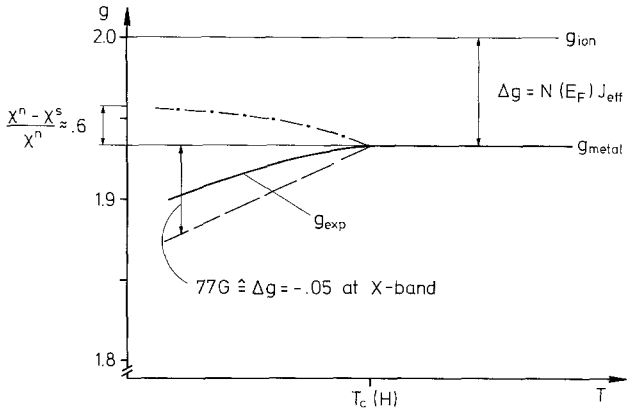

Fig. 7. Schematic diagram of the different effects which contribute to the experimentally determined g-value. If the local field is smaller than the external one a decrease (dashed line) would be observed. The bare reduction of the spin susceptibility is shown in the dashed-dotted line

Because of incomplete experimental results the full lineshape (at Q-band several 100 G) was attributed in previous papers to a convolution of the field distribution and one homogeneous line. From the foregoing we see that the field distribution yields only 10 (50) G for $CeRu_2$ ($LaOs_2$). Therefore only the central line can be a convolution of a homogeneous line of few Gauss and the distribution function $\rho(H_{\min} - H_V)$. We will come back to this point.

Another interesting question was to look for the change of the relaxation (homogeneous linewidth) in the superconducting phase. The ESR of a local moment seems to be a good tool to answer this question. In literature only few calculations exist on the spatial change of the order parameter in the vicinity of a local moment. Kümmel [36] calculated from the Bogoliubov equations with a paramagnetic impurity that the pair potential $\Delta(r)$ decreases markably over the region of some atomic distances from the impurity. Unfortunately this spatial variation of the pair potential is seen by the spin flip scattering electron only in a higher order approximation. Schlottmann showed that in a first Born approximation only the bulk potential is seen [43]: To create this local hole in the pair potential J^2 is needed. To scatter from infinity into the excited states of the potential hole and out, again J^2 is needed. The scattering on the local change of the pair potential therefore goes with J^6 and can be neglected in these experiments. Because of these arguments we assume that the electronic spin moment relaxes in the same way as a nuclear moment. The BCS theory shows that the relaxation below T_c is reduced by a factor of $\exp(-\Delta/k_B T)$. This was experimentally confirmed by many NMR experiments [37]. For $T = 0.5\ T_c$ the thermal broadening is reduced already by a factor of 10. This drastic reduction has the following consequence: In Chapter 2 we showed that the ESR spectrum of Gd with $S = 7/2$ contains a 7 linesspectra ($7/2 \leftrightarrow 5/2, \ldots, -7/2 \leftrightarrow -5/2$). The dynamics of this fine structure splitting caused by the crystalline electric field was calculated by Plefka [38] and Barnes [39] in the presence of the exchange interaction. A full resolved spectrum is only seen if the thermal broadening δ_{ie} is small compared to the crystal field splitting. In the opposite limit the theory predicts a narrowing of the fine structure; if $\delta_{ie} \gg$ crystal field splitting all seven lines collapse into a single line spectrum (exchange narrowing). This has mostly been detected for Gd in metals. For LaSbGd. Urban et al. [40] have shown both extremes: at 4 K a completely resolved and at 300 K a totally collapsed spectrum. In our case we suggest that the nonlorentzian part of the lineshape in Figures 3 and 4 is caused by this fine structure splitting. For several cubic intermetallic compounds it was possible to determine the crystal field parameters b_4 to be of the order of 20–60 G. This is of the same order of magnitude as the relaxation rate at T_c. An exponential decrease of this rate would stop the exchange narrowing. The total splitting between the $7/2 \leftrightarrow 5/2$ to $-7/2 \leftrightarrow -5/2$ transition ($H_0/100$) is roughly 500–1,000 G. Going from X-band to Q-band the intensity of the outer line increases relatively by a factor of 3–5 because of the change of the Boltzmann factor for the different levels. Also this is observed in both systems $CeRu_2$ and $LaOs_2$. Unfortunately all experiments up to now have been performed in polycrystalline (bulk and powder) samples. Therefore one has to average the angular dependent spectrum

$$P(\theta, \varphi) \propto 5/2\,\{\cos^4\theta + \sin^4\theta(\sin^4\varphi + \cos^4\varphi)\} - 3/2$$

over the sphere. A simulation of a fine structure spectrum for powder samples shows a broadening at the low- and highfield part. It also shows an increase of the broadening on lowering the temperature, but the agreement with the experiments was not very good. A possible explanation are the bulk samples we used: these are not ideal powders. Also the exchange narrowing of the $5/2 \leftrightarrow 3/2$ and $3/2 \leftrightarrow 1/2$ transition may cause a difference between the measured and calculated spectra.

In summary the experimental facts are the following:

1) The broadening of the resonance line in $CeRu_2$ and $LaOs_2$ for $T \ll T_c$ increases in changing the microwave frequency from X to K and Q-band.

2) The broadening in $LaOs_2$ is bigger than in $CeRu_2$.

3) An absolute amount of the broadening or splitting for $LaOs_2$ at $\nu \approx 35$ GHz and $T = 1.35$ K is approximately 800 G.

4) The central part of the spectrum still looks like a Dysonian line very similar to that in the normal conducting state.

5) In analysing this line we found a shift of the field for resonance (Figures 5 and 6).

6) The width of that line decreases drastically below T_c (Reference 4).

7) The smallest linewidth ($T \approx 1.3$ K) is approximately 26 G ($CeRu_2$) and 50 G ($LaOs_2$).

4.2. Supplementary Experiments

Passing the phase transition we checked the intensity of the resonance signal. Within the experimental error we did not find any change. This leads to the conclusion that in the superconducting phase the same number of Gd ions contribute to the resonance signal. This is in agreement with the skindepth (0.1 to 1 μ) [41] and the penetration depth λ (Table 3). Here the question rises: what is the number of vortices compared to the number of paramagnetic impurities? The upper and lower limit for the vortex distance d_{vor} is given by the penetration depth λ and the coherence length ξ_0. If the vortex distance becomes comparable to ξ_0, the cores overlap and the superconductivity breaks down. On the other hand if the vortex distance becomes bigger than the penetration depth λ one gets into the Meissner effect region. Using the numbers given in Table 3, we get the following result. The smallest vortex distance in our experiments is 100 Å, but most of the experiments are performed for vortex distances of 500–2,000 Å. On the other hand in an AB_2 lattice the distance d_{A-A} is given $d_{AA} = \sqrt{3}a/4$. If we assume a statistical distribution of the Gd ions we get

$$70\,\text{Å} > \bar{d}_{Gd} > 18\,\text{Å} \quad \text{(limits for 100 ppm and 1 \%)}.$$

Because of $d_{vor} \gg d_{Gd}$, the majority of the Gd ions cannot act as pinning centers. An additional proof of the assumption that the Gd ions are statistically distributed, were NMR experiments on ^{139}La in $LaOs_2$ [42]. We found a Knight shift dependent on the external field. At 13 kG $K^n \approx K^s$ and at low field $K^s \gg K^n$, in agreement with the ESR results (Fig. 6).
Different sample shape did not affect the resonance signal. Some of the experiments were performed with powder, others with bulk samples. Similar to NMR experiments we observed in the s.c. phase an increase of the (low frequency) noise. The effect was bigger the purer the samples; vortex motion might be an explanation.
The position of the resonance signal was very carefully observed for different sweeps of the external field. We did not detect any irreversibilities, and sweeping the field up or down did not affect the resonance position (any possible change of H_0 would be smaller than 1/10 of the line width).

5. Summary

The ESR of Gd and Eu in the normal conducting state of La metal and $LaAl_2$ can be related to the initial depression of the superconducting transition temperature. The resonance of these four systems shows a bottleneck behaviour. This enables us to determine directly the exchange spin-flip scattering rate of the conduction electrons at the magnetic impurity. To our knowledge this is the only direct technique which determines the scattering rate on a microscopic scale. The experimental results (Figure 2 and Table 1) agree very well with those determined from a T_c-measurement. A detailed analysis of the difference for Gd and Eu [16] will be published elsewhere. Doping an additional impurity (Ce or Th) into a bottleneck system, the effective (exchange plus s.o.) spin-flip scattering can be determined. For $\underline{La_xTh_{1-x}}Ce$, which is of current interest because of the reentrant behaviour and the demagnetisation of the Ce ion [26, 2], the ESR at Gd yields the mean free path for s.o. ($l_{s.o.}$) and exchange (l_{exch}) scattering. Alloying few percent Ce or Th into Lanthanum, we get: $2 \cdot l^{Ce}_{s.o.} \simeq l^{Ce}_{exch}$ and $4 \cdot l^{Th}_{s.o.} \simeq l^{Ce}_{s.o.}$.
Concerning the resonance in the superconducting phase, we present in this paper experimental data for 3 microwave frequencies and two hosts: $LaOs_2$ and $CeRu_2$, the only two which make those experiments possible (high T_c and H_{c2}). The experiments were performed in polycrystalline samples. The following interpretation is in agreement with all experimental facts and seems to be the most probable one:
We assume the bulk order parameter to be responsible for the relaxation rate δ_{ie}. Lowering the temperature to $T_c/2$ or more then would reduce the relaxation rate to 1/10 or more. This should stop the exchange narrowing. In a "single crystal" experiment a full resolved fine structure spectrum would be detectable (similar to $\underline{LaSb}Gd$, Reference 40). In an experiment with powder samples the low and high field part of the resonance is broadened due to the averaging of the angular dependent fine structure lines. This broadening is of the order of several hundred Gauss assuming a crystalline field parameter $b_4 \approx 50$ G [44, 45]. At $T \approx 1.5$ K and higher microwave frequencies the thermal population of the different Zeeman levels changes and the relative intensity of the central line decreases (the broadening increases). Consequently the central line in Figures 3 and 4 is interpreted to be a convolution of the field distribution and the $1/2 \leftrightarrow -1/2$ tran-

sitions. Again this is confirmed by the experiments. The smallest linewidth we were able to detect are 50 G ($LaOs_2$) and 26 G ($CeRu_2$). From Equation (14) and Table 3 one gets roughly the same values for the field distribution. The different g-values determined for the central line (Figures 5 and 6) are within the experimental error in agreement with the numbers given in Table 3. One gets a reduction of the conduction electron spin susceptibility of approx. 13%.

Final proof for this interpretation can be given only by a single crystal experiment. Unfortunately the high field superconductors are peritectic compounds and single crystals are very difficult to grow. If this interpretation holds the ESR of a localized moment in the superconducting phase would be a good tool (1) to stop the exchange narrowing and to determine the crystal field splitting; (2) to detect the resonance of those local moments, which show in normal conducting metals very strong relaxation rates (iron-group metals).

The author thanks Prof. Dr. S. Hüfner for his permanent interest in this work and encouragement, he thanks also all the members of the metal group, especially G. Koopmann, U. Engel, and W. Schrittenlacher. He is also indepted to Prof. Dr. B. Elschner who made the measurements at K-Band in his institute (THD) possible. Helpful discussions are acknowledged with Dr. S. Barnes, Dr. W. Brewer (who read the manuscript), Dr. D. Davidov, Dr. P. Monod as well as to Profs. Dr. B. Maple and Dr. R. Orbach who also sent preprints prior publication.

References

1. Buckel, W., Hilsch, R.: Z. Physik **128**, 324 (1950)
2. See for example: Maple, M.B.: In: Magnetism: A Treatise on Modern Theory and Materials (edited by Suhl, H.), vol. V, Chapter 10, London: Academic Press 1973
   Maple, M.B.: To be published
3. Rettori, C., Davidov, D., Chaikin, P., Orbach, R.: Phys. Rev. Lett. **30**, 437 (1973)
4. Engel, U., Baberschke, K., Koopmann, G., Hüfner, S., Wilhelm, M.: Sol. State Comm. **12**, 977 (1973)
5. Koopmann, G., Engel, U., Baberschke, K., Hüfner, S.: Sol. State Comm. **11**, 1197 (1972)
6. Rettori, C., Davidov, D., Orbach, R., Chock, E.P., Ricks, B.: Phys. Rev. B**7**, 1 (1973)
7. Abrikosov, A.A., Gor'kov, L.P.: Zh. Eksp. Teor. Fiz. **39**, 1781 (1960); Sov. Phys. JETP **12**, 1243 (1961)
8. Koopmann, G., Baberschke, K., Hüfner, S.: Phys. Lett. **50**A, 407 (1975)
9. Davidov, D., Chelkowski, A., Rettori, C., Orbach, R., Maple, M.B.: Phys. Rev. B**7**, 1029 (1973)
10. Orbach, R., Peter, M., Shaltiel, D.: Arch. Sc. Genève **27** (1974)
    Orbach, R.: Proc. of the 14th Conference on Low Temperature Physics (1975), Vol. 5 (edited by Krusius, M., and Vuorio, M.). Amsterdam: North-Holland, Pub. Comp. and references therein
11. Hasegawa, H.: Progr. Th. Phys. **21**, 483 (1959)
12. Zitkova-Wilcox, J.: Phys. Rev. B**7**, 3203 (1973)
13. Schäfer, W., Schmidt, H.K., Elschner, B., Buschow, K.H.J.: Z. Physik **254**, 1 (1972)
14. For a detailed discussion see for example Reference 2 and references therein
15. Watson, R.E.: In: Hyperfine Interactions (edited by Freeman, A.J., Frankel, R.B.) Chapter 9. London: Academic Press 1967
16. Koopmann, G.: Thesis (unpublished). FU Berlin (1975)
17. Yafet, Y.: J. Appl. Phys. **39**, 853 (1968); ibid. **42**, 1564 (1971) and Reference 10
18. Watson, R.E., Koida, S., Peter, M., Freeman, A.J.: Phys. Rev. **139**, A 167 (1963)
19. Schrieffer, J.R., Wolff, P.A.: Phys. Rev. **149**, 491 (1966)
20. Friedel, J.: Nuovo Cimento Suppl. **12**, 1861 (1958)
    Anderson, P.W.: Phys. Rev. **124**, 41 (1961)
21. Tao, L.J., Davidov, D., Orbach, R., Chock, E.P.: Phys. Rev. **134**, 5 (1971)
22. Murani, A.P.: Sol. State Comm. **13**, 85 (1973)
23. Davidov, D., Rettori, C., Chock, E.P., Orbach, R., Maple, M.B.: Proc. AIP No. 10, 138 (1972) Magnetism and Magnetic Materials
24. Müller-Hartmann, E., Zittartz, J.: Phys. Rev. Lett. **26**, 428 (1971)
    See also: Müller-Hartmann, E.: In Magnetism: A Treatise on Modern Theory and Materials, (edited by Suhl, H.) vol. V, chapter 12. London: Academic Press 1975
25. Cornut, B., Coqblin, B.: Sol. State Comm. **13**, 1171 (1973)
26. Huber, J.G., Fertig, W.A., Maple, M.B.: Solid State Comm. **15**, 453 (1974)
27. Davidov, D., Rettori, C., Baberschke, K., Chock, E.P., Orbach, R.: Phys. Lett. **45**A, 161 (1973)
28. Schrittenlacher, W., Baberschke, K., Koopmann, G., Hüfner, S.: Sol. State Comm. **16**, 923 (1975)
29. Engel, U.: Thesis (unpublished). FU Berlin (1974)
30. Davidov, D., Rettori, C., Kim, H.M.: Phys. Rev. B**9**, 147 (1974)
31. Lawson, A.C., Baberschke, K., Engel, U.: Phys. Lett. **48**A, 107 (1974)
32. For field distribution in the vortex state see textbooks on superconductivity e.g. Superconductivity Vol. 2, 840ff (edited by Parks, R.D.). New York: M. Dekker, Inc. 1969
    Orbach, R.: Phys. Letters **47**A, 281 (1974)
33. Davidov, D., Rettori, C., Baberschke, K., Orbach, R.: Phys. Letters **45**A, 163 (1973)
34. Anderson, P.W.: Phys. Rev. Lett. **3**, 325 (1959)
35. Baberschke, K., Engel, U., Hüfner, S.: Sol. State Comm. **15**, 1101 (1975)
36. Kümmel, R.: Phys. Rev. B**6**, 2617 (1972)
37. Silbernagel, B.G., Weyer, M., Wernick, J.E.: Phys. Rev. Letters **17**, 384 (1966)
38. Plefka, T.: Phys. stat. solidi (a) **55**, 129 (1973)
39. Barnes, S.E.: Phys. Rev. B**9**, 4789 (1974)
40. Urban, P., Davidov, D., Elschner, B., Plefka, T., Sperlich, G.: Phys. Rev. B**12**, 72 (1975)
41. Lawson, A.C., Engel, U., Baberschke, K.: Phys. Lett. **49**A, 373 (1974)
42. These experiments were performed together with Clark, W.G. at UCLA; unpublished
43. Schlottmann, P., FUB, private communication and to be published
44. Baberschke, K., Davidov, D., Rettori, C.: Proc. of the Low Temperature Conf. Vol. 3, p. 484, Helsinki (1975)
45. An ESR experiment on polycrystalline LaSb:Gd [40] showed the same broadening effects (P. Urban, private communication)

Klaus Baberschke
Institut für Atom- und Festkörperphysik
Freie Universität Berlin
Boltzmannstraße 20
D-1000 Berlin 33